Multi-dark-state resonances in cold multi-Zeeman-sublevel atoms

Bo Wang, Yanxu Han, Jintao Xiao, Xudong Yang, Changde Xie, and Hai Wang

The State Key Laboratory of Quantum Optics and Quantum Optics Devices, Institute of Opto-Electronics, Shanxi University, Taiyuan 030006, China

Min Xiao

The State Key Laboratory of Quantum Optics and Quantum Optics Devices, Institute of Opto-Electronics, Shanxi University, Taiyuan 030006, China, and Department of Physics, University of Arkansas, Fayetteville, Arkansas 72701

Received August 14, 2006; revised September 26, 2006; accepted September 26, 2006; posted September 28, 2006 (Doc. ID 74036); published November 22, 2006

We present our experimental and theoretical studies of multi-dark-state resonances (MDSRs) generated in a unique cold rubidium atomic system with only one coupling laser beam. Such MDSRs are caused by different transition strengths of the strong coupling beam connecting different Zeeman sublevels. Controlling the transparency windows in such an electromagnetically induced transparency system can have potential applications in multiwavelength optical communication and quantum information processing. © 2006 Optical Society of America

OCIS codes: 270.1670, 020.1670, 020.6580.

Since the early demonstrations of the electromagnetically induced transparency (EIT) phenomenon in various three-level atomic systems,[1–3] many new EIT-related phenomena have been discovered and studied.[4] One such interesting effect is dual-EIT or dual dark-state resonances studied in two coupled three-level EIT systems[5–9] or by perturbing one of the lower states in the three-level EIT systems (by using one additional optical or microwave field connecting to the fourth auxiliary energy level).[10–13] In those dual EIT systems, two transparency windows are created that can be used to allow transmissions of two probe beams simultaneously at two different wavelengths. The typical conditions for observing such dual dark-state resonances are four energy levels and three optical (or two optical and one microwave) fields. Although the two-photon Doppler-free condition allows the use of continuous-wave, low-power diode lasers to eliminate the first-order Doppler effect and makes it possible to observe EIT with relatively low coupling power,[3] the use of cold atoms can further reduce the power requirement for the coupling beam and allow narrow EIT windows.[14,15] The dual dark-state phenomenon was also observed in cold atoms by perturbing the lower state for the coupling transition in a three-level Λ-type system with a microwave field.[11] Also, the effects of degenerate Zeeman sublevels and various polarization configurations on EIT were studied in detail in a vapor cell or in cold atomic samples.[16–19]

In this Letter, we propose and experimentally demonstrate a new scheme to generate multi-dark-state resonances in a three-level (with multi-Zeeman sublevels) atomic system with only two laser fields. First, let us consider two atomic systems in ^{87}Rb atoms, as shown in Fig. 1. In Fig. 1(a), the linearly polarized coupling beam E_c (frequency ω_c) drives transition $5S_{1/2}$, $F=2$ to $5P_{1/2}$, $F'=1$. Since the transition strengths between different Zeeman levels are very close,[20] the Rabi frequencies (defined as $\Omega_{cij}=\mu_{ij}E_c/\hbar$, where μ_{ij} is the transition dipole moment with i,j denoting Zeeman sublevels) for different coupling transitions are almost equal. The linearly polarized probe beam will have a simple single-peak EIT as was studied extensively before.[15] However, when one chooses the up energy level to be $F'=2$ instead of $F'=1$, as shown in Fig. 1(b), the situation changes dramatically. Due to the large differences in

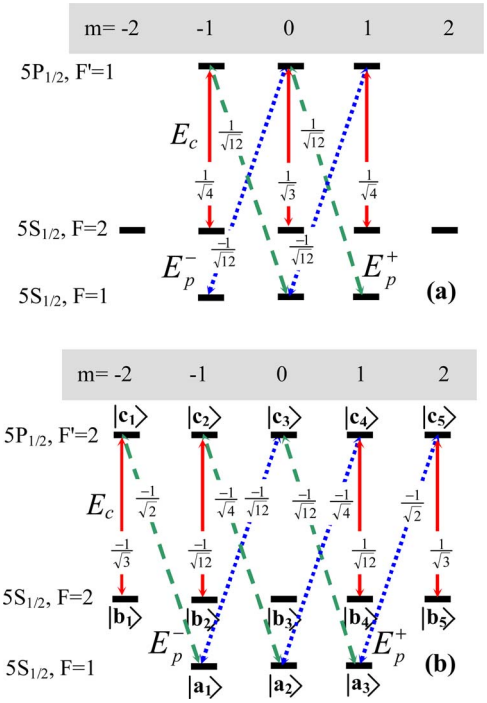

Fig. 1. (Color online) Λ-type EIT subsystems formed by linearly polarized probe and coupling fields (the polarizations of these two beams are perpendicular to each other) in $D1$ line of ^{87}Rb atoms. (a) Upper energy level is $5P_{1/2}$, $F'=1$; (b) Upper energy level is $5P_{1/2}$, $F'=2$.

0146-9592/06/243647-3/$15.00

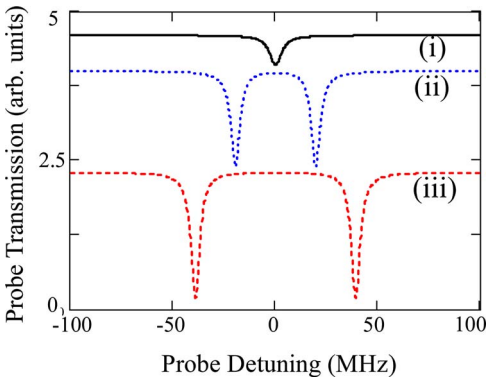

Fig. 2. (Color online) Absorption spectra of the probe field coupling to the upper Zeeman sublevel [for the system shown in Fig. 1(b)] of (i) $F'=2$, $m=0$, (ii) $F'=2$, $m=\pm1$, and (iii) $F'=2$, $m=\pm2$, respectively. Calculation parameters are $\Omega_{c22}=78$ MHz, $\Omega_p=2$ MHz, $\gamma_{ab}=40$ kHz, $\gamma_{ac}=2.8$ MHz (the curves have been vertically shifted for clarity).

the transition strengths for the coupling beam connecting different Zeeman sublevels, the Rabi frequencies for different Zeeman transitions are very different. For example, the effective Rabi frequencies for transitions $5S_{1/2}$, $F=2$, $m=\pm2$ to $5P_{1/2}$, $F'=2$, $m=\pm2$ are twice the values for the transitions $F=2$, $m=\pm1$ to $F'=2$, $m=\pm1$, respectively. Transition strength from $F=2$, $m=0$ to $F'=2$, $m=0$ is zero.[20] The effective Rabi splittings (in the dressed-state picture) for the upper energy levels ($F'=2$) have five split energy levels: $-\Omega_{c22}/2$, $-\Omega_{c11}/2$, 0, $+\Omega_{c11}/2$, and $+\Omega_{c22}/2$. In this particular system, $\Omega_{c22}=2\Omega_{c11}$. As the linearly polarized (perpendicular to the polarization of the coupling beam) probe field is scanned through these split energy levels, an absorption peak appears at the center frequency for the $F'=2$, $m=0$ transition (with probe fields Ω_{p3}^{-} connecting states $|a_3\rangle$ and $|c_3\rangle$ and Ω_{p1}^{+} connecting states $|a_1\rangle$ and $|c_3\rangle$) due to lack of EIT [as shown in curve (i) of Fig. 2]. The coupling field Ω_{c11} (connecting states $|b_2\rangle$ and $|c_2\rangle$) and Ω_{p2}^{-} (connecting states $|a_2\rangle$ and $|c_2\rangle$) form one EIT system, which is degenerate with another EIT system (formed by states $|a_2\rangle$, $|c_4\rangle$ and $|b_4\rangle$, with coupling field Ω_{c11} and probe field Ω_{p2}^{+}). Such an EIT system shows an EIT window with two absorption peaks at the positions of the dressed states, as shown in curve (ii) of Fig. 2. Similarly, coupling field Ω_{c22} (connecting states $|b_1\rangle$ and $|c_1\rangle$ as well as $|b_5\rangle$ and $|c_5\rangle$), together with probe fields Ω_{p1}^{-} (connecting states $|a_1\rangle$ and $|c_1\rangle$) and Ω_{p3}^{+} (connecting states $|a_3\rangle$ and $|c_5\rangle$), provides a larger EIT window, as shown in curve (iii) of Fig. 2. When these three curves in Fig. 2 are added together, the central absorption peak and the two absorption peaks in the first EIT curve cut the broad EIT window into four narrow EIT windows forming four separate dark-state resonances. Such multi-dark resonances are created by only one coupling laser beam. As the coupling field amplitude changes, the spaces and widths of these dark-state peaks will change accordingly.

We performed the experiment using ^{87}Rb atoms in a vapor-cell magneto-optical trap. The magneto-optical trap is similar to the ones used by others previously.[15–17] The diameter of the trapping beam is about 1 cm. The trapped ^{87}Rb atom cloud is $\sim$2 mm in diameter and contains $\sim10^9$ atoms at the temperature ~200 μK. The probe and coupling lasers are provided by two extended-cavity diode lasers with linewidth of $\sim$1.5 MHz. The probe laser frequency is scanned at a speed of 1.3 kHz/s across the $5S_{1/2}$, $F=1\rightarrow5P_{1/2}$, $F'=2$ transition and the frequency of coupling laser is locked to the $5S_{1/2}$, $F=2\rightarrow5P_{1/2}$, $F'=2$ transition. We choose the probe beam to be linearly polarized in the p direction (parallel to the optical table) and the coupling beam to be linearly polarized in the s direction (perpendicular to the optical table). The propagation directions between the probe beam and the coupling beam have an angle of $\sim$20°, and the diameters of the coupling beam and probe beam are $\sim$2.0 and $\sim$0.5 mm, respectively. Two beams overlap at the center of the cold atom cloud. During the experiment, the on–off sequence of the trapping, repumping, coupling, and probe beams is controlled by four acousto-optical modulators. The experiment is cycled at 10 Hz. In each cycle, the first 99 ms is used for cooling and trapping of the ^{87}Rb atoms. We switch on the coupling beam at the same time as we turn off the magneto-optical trap (trapping and repumping beams, as well as the magnetic field). 0.1 ms later, the probe beam is turned on and the transmitted probe beam from the cold atoms is detected by an avalance photodiode. Throughout the experiment a small magnetic field ($\sim$0.04 G) in the s direction defines the quantization axis of the atoms. So the coupling beam couples the Zeeman levels of $\Delta m=0$, while the probe beam couples the Zeeman levels of $\Delta m=\pm1$, with the left- and right-circularly-polarized components, as shown in Fig. 1(b).

Figure 3(a) plots the experimental results of probe

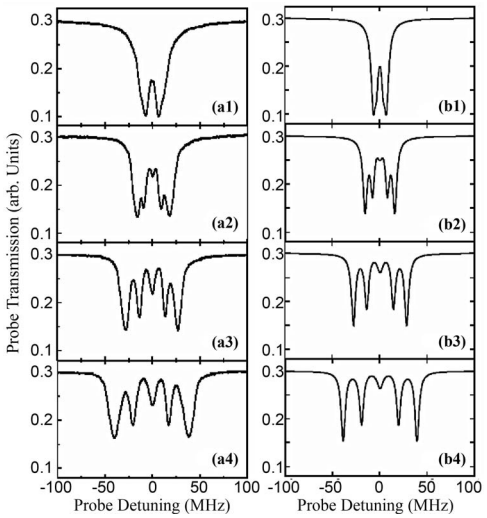

Fig. 3. (a) Multi-dark-state resonance spectra observed in the experiment. The probe beam Rabi frequency is $\Omega_p=2$ MHz, the coupling field Rabi frequencies in (a1)–(a4) are $\Omega_{c22}=14$, 31, 56, and 78 MHz, respectively. (b) Theoretical multi-dark-state resonance spectra calculated with the same parameters as in (a). Other parameters used in the calculation are $\gamma_{ab}=40$ kHz, $\gamma_{ac}=2.8$ MHz, laser linewidths = 1.5 MHz, $N=1\times10^{11}$ cm^{-3}.

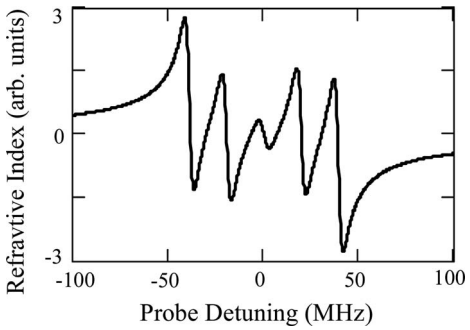

Fig. 4. Calculated probe dispersion with same parameters as in Fig. 3(b4).

transmission as a function of probe frequency detuning, which probes the dark-state structure of this system. When the coupling beam is relatively weak ($\Omega_{c22}=14$ MHz, with the probe beam Rabi frequency $\Omega_p=2$ MHz), the Zeeman sublevels are near degenerate, which gives a single EIT peak as shown in Fig. 3(a1). The absorption at the transition from $5S_{1/2}$, $F=1$, $m=0\rightarrow 5P_{1/2}$, $F'=2$, $m=0$ reduces the EIT effect and makes the total EIT dip smaller. As the coupling field amplitude increases to a larger value, several EIT windows start to appear at different probe frequencies with an absorption peak at the middle, as shown in Fig. 3(a2). A further increase of coupling power makes the split EIT windows clearer as given in Figs. 3(a3) and 3(a4).

The total probe field susceptibility is $\chi=\chi_1+\chi_2+\chi_3$, where χ_i $(i=1,2,3)$ are the sums of the left- and right-circularly-polarized probe field susceptibilities coming from contributions of the transitions $|a_i\rangle \rightarrow |c_i\rangle$ and $|a_i\rangle\rightarrow|c_{i+2}\rangle$, respectively. These susceptibilities can be expressed in the following compact form[21]:

$$\chi_i = -\frac{N}{\hbar\epsilon_0}\left(\frac{|\mu_{c_i,a_i}|^2}{\Omega^-_{p_i}}\rho_{a_i,c_i}+\frac{|\mu_{c_{6-i},a_{4-i}}|^2}{\Omega^+_{p_{4-i}}}\rho_{a_{4-i}c_{6-i}}\right); \quad (1)$$

ρ_{a_i,c_i} and $\rho_{a_{4-i},c_{6-i}}$ can be calculated by solving the density-matrix equations involving all Zeeman sublevels in the system.[21] N is the atomic density. Figure 3(b) plots the theoretical multi-dark-state resonance spectra calculated with the same parameters as in Fig. 3(a). One can see that the agreements between these experimentally measured curves and theoretically calculated ones are excellent.

The frequencies of these multi-EIT windows (or dark states) can be controlled by the coupling beam power, which allows transmissions of the probe beam at different frequencies. Such tunable EIT windows can be used for multichannel optical communication or quantum information processing. With such sharp EIT windows, probe photons at different frequencies can be slowed down simultaneously. Figure 4 depicts the dispersion property for the case of large coupling beam strengths. As one can see, sharp normal dispersions appear at different frequencies and can be used to modify group velocities of the probe beams at different frequencies.

In conclusion, we have demonstrated multi-dark resonances in a unique multi-Zeeman-sublevel atomic system in cold atoms with only one coupling beam. The differences in coupling Rabi frequencies due to different transition strengths among different Zeeman sublevels, together with the absorption peak at $m=0$ transition, split the broad EIT window into four narrow EIT windows, which are controllable by coupling beam power. Such an interesting effect only occurs in unique atomic systems with certain Zeeman sublevels and can be observed only in cold atoms. Such controllable multiple EIT windows can be used for multichannel optical communication and multichannel quantum information processing.

We acknowledge funding support by the National Natural Science Foundation of China (60325414, 60578059, 60238010, and RGC60518001). Corresponding author H. Wang's e-mail address is wanghai@sxu.edu.cn.

References

1. S. E. Harris, Phys. Today **50**(7), 36 (1997).
2. K. J. Boller, A. Imamoglu, and S. E. Harris, Phys. Rev. Lett. **66**, 2593 (1991).
3. J. Gea-Banacloche, Y. Li, S.-Z. Jin, and M. Xiao, Phys. Rev. A **51**, 576 (1995).
4. M. D. Lukin and A. Imamoglu, Nature (London) **413**, 273 (2001).
5. E. Paspalakis and P. L. Knight, Phys. Rev. A **66**, 015802 (2002).
6. D. Petrosyan and Y. P. Malakyan, Phys. Rev. A **70**, 023822 (2004).
7. S. Rebic, D. Vitali, C. Ottaviani, P. Tombesi, M. Artoni, F. Cataliotti, and R. Corbalán, Phys. Rev. A **70**, 032317 (2004).
8. A. Joshi and M. Xiao, Phys. Rev. A **71**, 041801 (2005).
9. C. Goren, A. D. Wilson-Gordon, M. Rosenbluh, and H. Friedmann, Phys. Rev. A **69**, 063802 (2004).
10. C. Wei and N. B. Manson, Phys. Rev. A **60**, 2540 (1999).
11. Y.-C. Chen, Y.-A. Liao, H.-Y. Chiu, J.-J. Su, and I. A. Yu, Phys. Rev. A **64**, 053806 (2001).
12. S. F. Yelin, V. A. Sautenkov, M. M. Kash, G. R. Welch, and M. D. Lukin, Phys. Rev. A **68**, 063801 (2003).
13. C. Y. Ye, A. S. Zibrov, Y. V. Rostovtsev, and M. O. Scully, Phys. Rev. A **65**, 043805 (2002).
14. S. A. Hopkins, E. Usadi, H. X. Chen, and A. V. Durrant, Opt. Commun. **138**, 185 (1997).
15. M. Yan, E. Rickey, and Y. Zhu, J. Opt. Soc. Am. B **18**, 1057 (2001).
16. Y.-C. Chen, C.-W. Lin, and I. A. Yu, Phys. Rev. A **61**, 053805 (2000).
17. J. Wang, Y. Zhu, K. J. Jiang, and M. S. Zhan, Phys. Rev. A **68**, 063810 (2003).
18. R. Wynands, A. Nagel, S. Brandt, D. Meschede, and A. Weis, Phys. Rev. A **58**, 196 (1998).
19. D. Petrosyan and G. Kurizki, Phys. Rev. A **65**, 033833 (2002).
20. For details of the transition probabilities of $D1$ line in ^{87}Rb, see http://steck.us/alkalidata.
21. B. Wang, S. Li, J. Ma, H. Wang, K. C. Peng, and M. Xiao, Phys. Rev. A **73**, 051801(R) (2006).